⌘ *Author's Choice*

THE JOURNAL OF BIOLOGICAL CHEMISTRY VOL. 286, NO. 37, pp. 32834–32842, September 16, 2011

Comparative Analysis of *Histophilus somni* Immunoglobulin-binding Protein A (IbpA) with Other Fic Domain-containing Enzymes Reveals Differences in Substrate and Nucleotide Specificities*[S]

Received for publication, February 2, 2011, and in revised form, July 23, 2011 Published, JBC Papers in Press, July 27, 2011, DOI 10.1074/jbc.M111.227603

Seema Mattoo[‡1], Eric Durrant[§], Mark J. Chen[¶], Junyu Xiao[§], Cheri S. Lazar[§], Gerard Manning[¶], Jack E. Dixon[‡§], and Carolyn A. Worby[§2]

From the [‡]Howard Hughes Medical Institute and Department of Pharmacology and the [§]Departments of Pharmacology, Cellular and Molecular Medicine, and Chemistry and Biochemistry, University of California, San Diego, La Jolla, California 92093-0721 and the [¶]Razavi Newman Center for Bioinformatics, Salk Institute, La Jolla, California 92037

A new family of adenylyltransferases, defined by the presence of a Fic domain, was recently discovered to catalyze the addition of adenosine monophosphate (AMP) to Rho GTPases (Yarbrough, M. L., Li, Y., Kinch, L. N., Grishin, N. V., Ball, H. L., and Orth, K. (2009) *Science* 323, 269–272; Worby, C. A., Mattoo, S., Kruger, R. P., Corbeil, L. B., Koller, A., Mendez, J. C., Zekarias, B., Lazar, C., and Dixon, J. E. (2009) *Mol. Cell* 34, 93–103). This adenylylation event inactivates Rho GTPases by preventing them from binding to their downstream effectors. We reported that the Fic domain(s) of the immunoglobulin-binding protein A (IbpA) from the pathogenic bacterium *Histophilus somni* adenylylates mammalian Rho GTPases, RhoA, Rac1, and Cdc42, thereby inducing host cytoskeletal collapse, which allows *H. somni* to breach alveolar barriers and cause septicemia. The IbpA-mediated adenylylation occurs on a functionally critical tyrosine in the switch 1 region of these GTPases. Here, we conduct a detailed characterization of the IbpA Fic2 domain and compare its activity with other known Fic adenylyltransferases, VopS (*Vibrio* outer protein S) from the bacterial pathogen *Vibrio parahaemolyticus* and the human protein HYPE (huntingtin yeast interacting protein E; also called FicD). We also included the Fic domains of the secreted protein, PfhB2, from the opportunistic pathogen *Pasteurella multocida*, in our analysis. PfhB2 shares a common domain architecture with IbpA and contains two Fic domains. We demonstrate that the PfhB2 Fic domains also possess adenylyltransferase activity that targets the switch 1 tyrosine of Rho GTPases. Comparative kinetic and phylogenetic analyses of IbpA-Fic2 with the Fic domains of PfhB2, VopS, and HYPE reveal important aspects of their specificities for Rho GTPases and nucleotide usage and offer mechanistic insights for determining nucleotide and substrate specificities for these enzymes. Finally, we compare the evolutionary lineages of Fic proteins with those of other known adenylyltransferases.

The bacterial pathogen *Histophilus somni* produces a large surface antigen called immunoglobulin-binding protein A (IbpA)[3] that is expressed on the cell surface via a two-partner secretion system (1). IbpA contains filamentous hemagglutinin and coiled coil domains in the amino terminus along with two filamentation induced by cAMP (Fic) domains and a YopT-like cysteine protease domain in the carboxyl terminus. The *H. somni* Fic domains catalyze an adenylylation reaction where adenosine triphosphate (ATP) is hydrolyzed to add an adenosine monophosphate (AMP) to the tyrosine in the switch 1 region of Rho family guanosine triphosphatases (GTPases), RhoA, Rac, and Cdc42, thereby blocking their ability to bind to downstream effectors (2).

The covalent addition of AMP to proteins has been previously described. In the 1960s, bacterial glutamine synthetase was reported to be stably adenylylated on up to 12 tyrosine residues, with the degree of adenylylation controlling enzymatic activity (3). Transient adenylylation of the C-terminal glycine or the catalytic lysine also occurs during the activation of ubiquitin and ubiquitin-like proteins as well as during DNA and RNA ligation processes (4, 5). These transient adenylylation events serve chiefly as priming reactions with the hydrolysis of the high energy phosphate bonds in ATP providing the necessary energy for the subsequent reactions. Fic proteins are not homologous to bacterial glutamine-synthetase adenylyltransferase (GS-ATase), the polynucleotide ligases, or the E1-like enzymes. Recently, another bacterial effector, *Legionella pneumophila* DrrA, was shown to adenylylate a Tyr residue in the switch 2 region of Rab1b (6). DrrA does not contain a Fic motif but instead bears structural similarity to bacterial GS-ATases.

We previously demonstrated that adenylylation of Rho GTPases by IbpA Fic domains requires the conserved histidine in the core motif of the Fic domain, HPF*XX*GNGR, as mutating the histidine to alanine nearly eliminates adenylyltransferase (ATase) activity and prevents cytotoxicity (2). Adenylylated

* This work was supported, in whole or in part, by National Institutes of Health Grants GM090328 (to J. E. D.) and HG04016 (to G. M.).

⌘ *Author's Choice*—Final version full access.

[S] The on-line version of this article (available at http://www.jbc.org) contains supplemental Tables 1 and 2 and Figs. 1–3.

[1] To whom correspondence may be addressed: 9500 Gilman Dr., MC 0721, La Jolla, CA 92093-0721. Fax: 858-822-5888; E-mail: smattoo@ucsd.edu.

[2] To whom correspondence may be addressed: 9500 Gilman Dr., MC 0721, La Jolla, CA 92093-0721. Fax: 858-822-5888; E-mail: cworby@ucsd.edu.

[3] The abbreviations used are: IbpA, immunoglobulin-binding protein A; VopS, *Vibrio* outer protein S; ATase, adenylyltransferase; GS-ATase, glutamine-synthetase ATase; HYPE, huntingtin yeast interacting protein E; SUMO, small ubiquitin-like modifier; Ni^{2+}-NTA, Ni^{2+}-nitrilotriacetic acid; GDI, GDP dissociation inhibitor; PAK, p21-activated kinase; GMP-PNP, 5′-guanylyl imidodiphosphate; Fic, filamentation induced by cAMP.

Rho GTPases have also been reported to retract the cytoskeleton in bovine alveolar type 2 (BAT2) cells, allowing *H. somni* to cross the alveolar barrier and cause septicemia (7).

Other Fic domain-containing proteins, such as VopS (*Vibrio* outer protein S) from *Vibrio parahaemolyticus,* have been shown to adenylylate Rho GTPases on a nearby conserved threonine residue in the switch 1 region (8). IbpA and VopS do not share sequence similarities other than the conserved Fic core motif, but they do share significant structural similarity (8, 9). We recently solved the structure of the IbpA Fic2 domain in complex with Cdc42 (Protein Data Bank (PDB): 3N3V) (9). This structure reveals that IbpA-Fic2 contains an NH_2-terminal extension, which we refer to as an "arm segment," which recognizes a three-dimensional epitope in the Rho family proteins involving their switch 1 and switch 2 regions, resulting in tight substrate specificity. Consistent with our structure, the recently published VopS structure (PDB: 3LET) also contains an arm-like segment (8). Superimposing VopS onto IbpA-Fic2 suggests that this arm is in a perfect position to interact with the switch 2 region of Cdc42 (9). As mentioned above, VopS adenylylates a Thr rather than a Tyr residue in the switch 1 region. The significance of Tyr *versus* Thr adenylylation is currently unclear as both modifications serve to block downstream signaling by the GTPases (2, 10). Another secreted Fic protein, AnkX from *L. pneumophila*, has been implicated in breakdown of the Golgi network, although an ATase activity and substrate have not been identified for it (11). In addition, a single Fic domain-containing protein, HYPE (huntingtin yeast interacting protein E; also called FicD), exists in humans. HYPE and its *Drosophila* homolog have also been demonstrated to possess ATase activity (2, 12). Several other Fic domain structures have been solved by structural genomics efforts (PDB 2F6S, 2G03, 3CUC, 3EQX, 2JK8, and 2VZA); all contain variations on the conserved core Fic domain, but none contain the arm segment common to IbpA and VopS (9, 13). Not unexpectedly, although many of these enzymes autoadenylylate, they fail to adenylylate Rho GTPases, making their cellular substrates of paramount interest (9, 14).

Fic proteins are evolutionarily related to the toxin Doc (death on curing), a component of the toxin-antitoxin module encoded by the *phd/doc* operon in P1 bacteriophage (15). Doc is a ribosomal toxin that binds and inhibits the 30 S ribosomal subunit in a manner similar to hygromycin (16). Although an adenylyltransferase activity for Doc has not been demonstrated, the histidine of the Doc Fic motif is important for its ability to function as a ribosomal toxin (15). Fic proteins bear significant sequence and structural similarity to P1 bacteriophage Doc. As such, Fic and Doc-like proteins have been recently classified as the FiDo (Fic/Doc) family (12).

Over 4300 proteins contain a Fic domain (InterPro database). Is the presence of a Fic domain sufficient to confer ATase activity? What other substrates do Fic proteins target? Finally, does the variability in the Fic motif sequence dictate substrate specificity, or perhaps specificity for nucleotide usage? In this study, we have attempted to answer these questions while conducting a detailed enzymatic characterization of IbpA-Fic2. First, we demonstrate that another Fic protein, the *Pasteurella multocida* secreted virulence factor PfhB2 (*Pasteurella* filamentous hemagglutinin B2), also adenylylates Rho GTPases in a manner similar to IbpA. We, further, compare the ATase activity of the Fic domains of *H. somni* IbpA, *P. multocida* PfhB2, *V. parahaemolyticus* VopS, and human HYPE and find that VopS displays the ability to effectively use a nucleotide other than ATP as a co-substrate. This finding greatly broadens our appreciation for the scale of post-translational modifications carried out by the Fic family of enzymes. Using mutant proteins with chimeric Fic motifs, we address the role of the Fic motif sequence in determining substrate and nucleotide specificities and conduct a phylogenetic analysis to understand the functional evolution of these proteins. Finally, we determine the catalytic parameters for the IbpA-Fic adenylylation of a constitutively active form of Cdc42 and compare our results with those determined for VopS.

EXPERIMENTAL PROCEDURES

Cloning, Protein Expression, and Purification—Rho GTPase clones were obtained from the Missouri S&T cDNA Resource Center. GST fusion, His-SUMO fusion, and MBP-His-TEV fusion proteins were expressed in *Escherichia coli* BL21 RILP (Stratagene) in LB medium containing 100 μg/ml ampicillin (pET-GSTx and pSJ8) or kanamycin (pSMT3) to a density of 0.6 A_{600}. Protein expression was induced overnight at room temperature with 0.4 mM isopropyl-β-D-thiogalactopyranoside. Cells were lysed in 20 mM Hepes, pH 7.4, 100 mM NaCl, 0.5 mM tris(2-carboxyethyl)phosphine, and protease inhibitors by sonication and affinity-purified using GST-Bind resin (Novagen) or Ni^{2+}-NTA resin (Qiagen). The His_6-SUMO tag and MBP-His-TEV tags were cleaved using recombinant ULP1 and tobacco etch virus proteases, respectively. The affinity tags were then removed by passing the proteins over Ni^{2+}-NTA resin a second time. Protein concentrations were measured using the Bradford method, purity was determined by SDS-PAGE, and proteins were stored at −80 °C.

In Vitro Adenylylation and Nucleotide Exchange Assays—Approximately 5 μg of GST-IbpAFic1, GST-IbpAFic2, GST-PfhB2Fic1, GST-PfhB2Fic2, and GST-HYPE were incubated with 5 μg of GST-RhoA, Rac, or Cdc42 or their Gly, Thr, or Tyr mutants in 40-μl adenylylation reactions containing 25 mM Tris-HCl (pH 7.5), 3.0 mM $MgCl_2$, 1 mM DTT, 0.5 mM EDTA, and 5 μCi of [α-^{32}P]ATP for 30–60 min at 30 °C. Reactions were stopped with NuPAGE loading buffer (Invitrogen).

Nucleotide loading and GTPase activation assays were carried out as described previously (17) using untagged RhoA, Rac1, and Cdc42. RhoGDI binding and subsequent *in vitro* adenylylation reactions were carried out by transfecting HEK293A cells with HA-tagged RhoA, Rac1 or Cdc42. After recovering for 48 h, cells were lysed in 600 μl of 50 mM Tris-Cl, pH 7.2, 1% (w/v) Triton X-100, 500 mM NaCl, 0.2 mM PMSF, and a protease inhibitor mixture. HA-tagged GTPases were loaded with GDP or GMP-PNP (17). Nucleotide exchange was confirmed by assessing the ability of GDP- or GMP-PNP-bound GTPases to bind to GST-Rhotekin or GST-PAK (17), as assessed by Western blot using antibodies against RhoA, Rac1, and Cdc42 (BD Transduction Laboratories).

His_6-SUMO-RhoGDI beads were added to the GDP or GMP-PNP loaded GTPases, and the samples were rotated for

2 h at 4 °C. Beads were washed three times with 1 ml of lysis buffer and once with 1× adenylylation reaction buffer. The adenylylation reaction was carried out as described above in the presence of 10 mM cold ATP. After 30 min, the beads were pelleted, and the supernatant and bead fractions were saved. The bead fractions were then washed three times with 1 ml of 50 mM Tris-Cl, pH 7.2, 1% (w/v) Triton X-100, 150 mM NaCl, 10 mM $MgCl_2$, 0.2 mM PMSF containing protease inhibitors. The HA-Rho GTPase-RhoGDI complex was eluted with wash buffer containing 300 mM imidazole. Laemmli loading buffer was added to the bead eluate and to the previously collected supernatant fraction, and the samples were separated on AnyKD gels (Bio-Rad). The separated proteins were then transferred to nitrocellulose and subjected to autoradiography. Protein load was visualized by Ponceau S staining.

For nucleotide specificity assays, *in vitro* reactions were conducted as above with α-^{32}P-labeled ATP, GTP, CTP, UTP, or dTTP (PerkinElmer Life Sciences) containing 1 mM of each respective cold dNTP. Adenylylation was visualized by autoradiography at various exposures.

Kinetic Data Analysis—The adenylylation of Cdc42-Q61L by IbpA-Fic2 was assayed using [α-^{32}P]ATP (PerkinElmer Life Sciences) and P81 Whatman filter paper. The reaction buffer consisted of 20 mM Hepes, pH 7.4, 100 mM NaCl, 1 mg/ml BSA, 0.5 mM tris(2-carboxyethyl)phosphine, 5 μCi of [α-^{32}P]ATP, and equal concentrations of ATP and $MgCl_2$. Reactions were performed at 25 °C in triplicate for 120 s. The reaction was initiated with 0.56 nM IbpA-Fic2, in a final volume of 25 μl, and stopped with an equal volume of stop solution (0.1 M EDTA, 0.1 M ATP). 25 μl of the stopped reaction were immediately pipetted onto P81 Whatman filter paper and dropped into a beaker containing 500 ml of 0.4% phosphoric acid that was sitting on a rotating platform. The filters were washed 30 min with 0.4% phosphoric acid (500 ml/wash) for a total of four washes followed by a final wash of 95% ethyl alcohol. Afterward, the filters were allowed to air dry before being placed in scintillation vials followed by counting in a Beckman LS 6000IC scintillation counter. To analyze the apparent kinetic values (K_m) of ATP using Fic2 with Cdc42-Q61L, the substrate concentration was held constant at 500 μM while varying the ATP concentration with equal molar $MgCl_2$, 0.1–10 mM. To determine the k_m for Cdc42-Q61L, the ATP and $MgCl_2$ concentrations were held at 5 mM, and substrate concentration was varied from 0.10 to 2.8 mM.

The kinetic values were fitted with the Michaelis-Menten equation (Equation 1) using GraphPad Prism 4

$$v = \frac{V_{max}[S]}{K_m + [S]} \quad \text{(Eq. 1)}$$

where V_{max} represents the maximum velocity, S is the substrate concentration, and K_m is the substrate concentration at half of the maximum velocity.

Computational and Phylogenetic Analyses—The domain profiles of IbpA, PfhB2, VopS, and HYPE were analyzed using the SMART database. Fic domains were aligned with the PROMALS3D server using the PDB coordinates of the IbpA-Fic2 structure (PDB 3N3U). For phylogenetic analyses, the sequence homologs of each individual group were selected from the collection of Fic proteins using PSI-BLAST and hidden Markov model searches of the National Center for Biotechnology Information (NCBI) peptide non-redundant (NR protein) database. Sequences of each group designated in supplemental Table 1 were aligned with PROMALS3D followed by manual adjustment. Accession IDs for the proteins used in this analysis are provided as part of supplemental Table 2. The alignment of the GS-ATase-KN-DrrA group was edited based upon DaliLite alignment of their structures. The phylogenetic tree of each group was inferred using the neighbor joining method in MEGA version 5. Neighbor joining analyses were done using Poisson correction methods, pairwise deletion of gaps, 1000 bootstrap replicates, and the default assumptions of homogenous substitution rates among sites and between lineages. Mid-point rooting was used for each tree.

RESULTS AND DISCUSSION

Alignment of the Fic Domains of IbpA with PfhB2, VopS, and HYPE—We characterized the enzymatic activity of the IbpA Fic2 domain as it compares with other enzymatically active Fic domains, such as *H. somni* IbpA-Fic1, *V. parahaemolyticus* VopS, and human HYPE (supplemental Fig. 1*A*). We also included the Fic domains of *P. multocida* PfhB2 in this analysis. The PfhB2 Fic1 and Fic2 domains share 64% amino acid sequence identity with IbpA-Fic1 and -Fic2, respectively, but have not been shown to function as ATases. Supplemental Fig. 1*B* shows an alignment of the Fic domains of IbpA (Fic1, amino acids 2994–3358, and Fic2, amino acids 3359–3781); PfhB2 (Fic1, amino acids 2892–3191, and Fic2, amino acids 3309–3609); VopS, amino acids 30–388; and HYPE, amino acids 181–458 and their predicted secondary structure as compared with the structure for IbpA-Fic2 (PDB 3N3U and 3N3V) (9). Despite their low sequence similarity, each of these Fic domains shares a common structural fold consisting of seven α-helices (α8–α14), with a surface-exposed loop containing the Fic H*X*F*XX*(G/A)N(G/K)R motif. In addition, IbpA-Fic2 residues shown to be critical for binding to ATP (supplemental Fig. 1*B*, *red arrows*) and to the switch 1 and switch 2 regions of Rho GTPases (supplemental Fig. 1*B*, *blue* and *black arrows*, respectively) are conserved between IbpA and PfhB2 (9).

Substrate Specificity of Fic Proteins against Rho GTPase Substrates—IbpA-Fic2 and HYPE have been shown *in vitro* to target the conserved switch 1 Tyr-32 of Cdc42 and Rac1 and Tyr-34 of RhoA (2). In contrast, VopS has been demonstrated to target the conserved switch 1 Thr-35 of Cdc42 and Rac1 and Thr-37 of RhoA (10). We, therefore, tested the ability of the Fic domains described in supplemental Fig. 1 to target Rho GTPases, RhoA, Rac1, and Cdc42 and their switch 1 mutants to determine whether they targeted Rho GTPases, and if so, which residue. IbpA-Fic1, IbpA-Fic2, PfhB2-Fic1, PfhB2-Fic2, and VopS were purified as GST fusions using glutathione-Sepharose. HYPE-Fic was purified as a His_6-SUMO fusion. These purified Fic proteins were then incubated with GST-tagged and purified RhoA, Rac1, and Cdc42 in an *in vitro* adenylylation reaction. Results with Cdc42 as a substrate are shown (Fig. 1*A*). As expected, IbpA-Fic1, IbpA-Fic2, and HYPE-Fic adenylylated

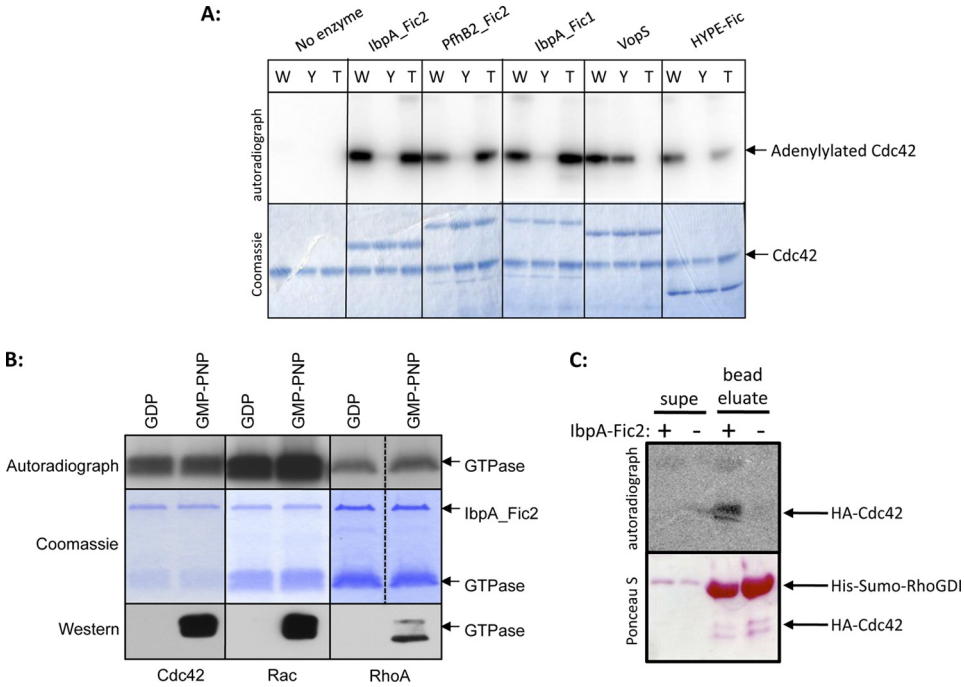

FIGURE 1. **Substrate specificity of IbpA-Fic2.** *A*, the Fic domains of IbpA, PfhB2 and HYPE target Tyr-32 of Cdc42, whereas VopS targets Thr-35. Bacterially expressed GST-tagged IbpA-Fic2, IbpA-Fic1, PfhB2-Fic2, VopS, or HYPE-Fic was incubated with wild type (*W*), Y32F (*Y*) or T35A (*T*) versions of Cdc42 expressed as GST fusion proteins in bacteria in an *in vitro* adenylylation assay using [α-^{32}P]ATP. Samples were separated on SDS-PAGE and visualized by autoradiography (*top panel*) and Coomassie Blue staining (*bottom panel*). The position of Cdc42 on the gel is indicated by *arrows*. The Fic domains of IbpA, PfhB2, and HYPE adenylylate wild type Cdc42 and Cdc42-T35A but not Cdc42-Y32F, indicating their specificity for the switch 1 tyrosine. In contrast, VopS fails to adenylylate only Cdc42-T35A, indicating its specificity for the switch 1 threonine. *B*, IbpA-Fic2 targets both the active and the inactive forms of Rho GTPases. Bacterially expressed untagged Cdc42, Rac, and RhoA loaded with GDP or GMP-PNP (as described under "Experimental Procedures") were incubated with IbpA-Fic2 in an *in vitro* adenylylation assay. The protein load was visualized by Coomassie Blue staining, and the amount of adenylylation was visualized by autoradiography. The nucleotide status of the GTPases was confirmed prior to adenylylation by incubation with GST-Pak (Cdc42 and Rac) or GST-Rhotekin (RhoA) followed by separation on SDS-PAGE and Western analysis using antibodies directed against the individual GTPases. *C*, IbpA-Fic2 is active against the Cdc42-RhoGDI complex. HA-tagged Cdc42 was expressed in HEK293A cells. Bacterially expressed His_6-SUMO-RhoGDI bound to nickel-agarose beads was incubated with the HEK239A cell extract treated for GDP loading of Rho GTPases (as described under "Experimental Procedures.") to allow Cdc42-RhoGDI complex formation. After washing, the beads were subjected to the *in vitro* adenylylation reaction in the presence or absence of GST-tagged IbpA-Fic2. The supernatant (*supe*) and bead eluate were separated on SDS-PAGE and visualized by autoradiography. The protein load was monitored by Ponceau S staining.

wild type Cdc42 and its Thr-35 to Ala mutant, but not the Tyr-32 to Phe mutant. Likewise, VopS adenylylated the wild type and the Tyr-32 to Phe mutant of Cdc42, but not the Thr-35 to Ala mutant. Both Fic domains of PfhB2 displayed ATase activity against Cdc42 (Fig. 1*A* and data not shown), specific to Tyr-32. This is the first demonstration of ATase activity for PfhB2. Together, these data confirm that IbpA, PfhB2, and HYPE function as tyrosyl ATases, whereas VopS functions as a threonine-specific ATase. Given that Tyr-32 and Thr-35 are in such close proximity and that the arm segment of each of the Fic proteins likely serves as a docking site for Cdc42, it is plausible that these proteins would modify any available free hydroxyl group in the Cdc42 switch 1 region. Our data indicate that this is not the case. These data further indicate that Tyr-32 and Thr-35 are the only Cdc42 residues that are targeted for adenylylation by the Fic domains of IbpA, PfhB2, HYPE, and VopS. Similar results were obtained with RhoA and Rac1 (supplemental Fig. 2, *A* and *B*, respectively).

IbpA-Fic2 Targets Both the Active and the Inactive Forms of Rho GTPases—To determine whether IbpA-Fic2 displays a substrate preference for the active (GTP-bound) or inactive (GDP-bound) form of the GTPases, we performed *in vitro* adenylylation reactions on bacterially expressed wild type untagged RhoA, Rac1, and Cdc42 loaded with either GDP or the non-hydrolyzable GTP analog, GMP-PNP. To confirm the efficiency of nucleotide exchange, GDP or GMP-PNP loaded GTPases were tested for the ability to bind to downstream effectors, Rhotekin, or PAK. Only the active (GMP-PNP-bound) forms of RhoA, Rac and Cdc42, bound to Rhotekin and PAK, respectively, as determined by Western blot analysis (Fig. 1*B*). Further, IbpA-Fic2 was capable of adenylylating both the active and the inactive forms of these GTPases, as determined by autoradiography (Fig. 1*B*). This result is in agreement with our crystallographic data where IbpA-Fic2 co-crystallized with an adenylylated, GDP-bound form of Cdc42 (PDB: 3N3V) (9). This result contradicts previously reported observations where IbpA-Fic2 targeted only the active forms of the GTPases in HeLa cells following transfection with point mutants that lock the GTPases into constitutively active (G12V/G14V) or dominant negative (T17N/T19N) conformations (2, 10). We reconcile this discrepancy by inferring that the inactivating point mutations used in the earlier assays altered the conformation of the GTPases, such that they may not be effectively recognized by the arm domain of IbpA-Fic2.

IbpA-Fic2 Is Active against the Rho GTPase-RhoGDI Complex—Small GTPases cycle between an inactive, GDP-bound and active, GTP-bound state. Three families of proteins regulate this switching of molecular states, namely GTPase exchange factors, GTPase-activating proteins, and GDP dissociation inhibitors (GDIs) (18). GTPase exchange factors act as

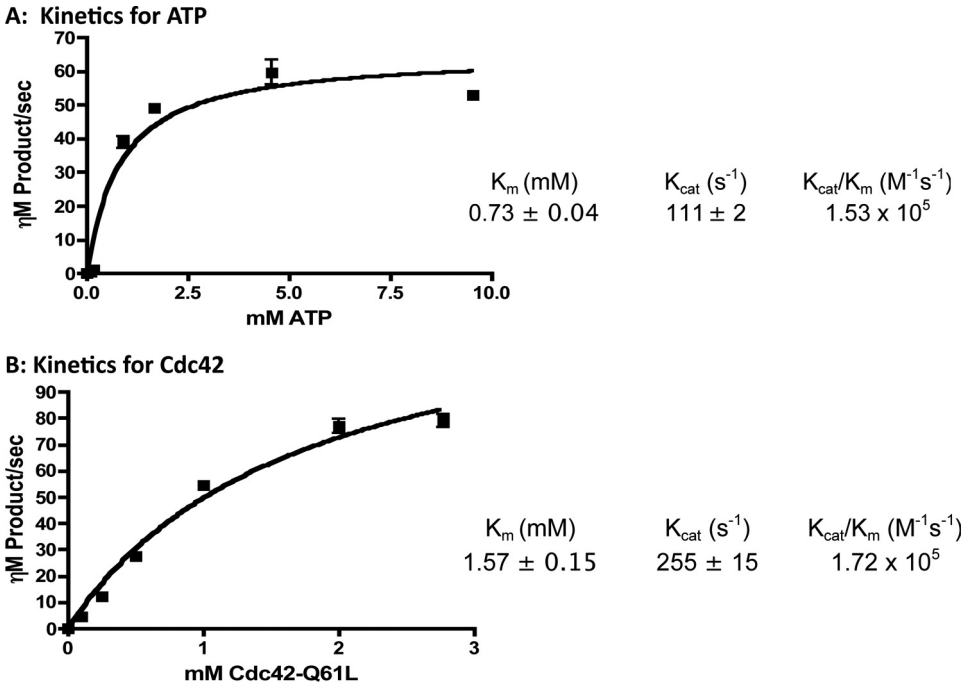

FIGURE 2. **Apparent steady-state kinetic measurements for ATP and constitutively active Cdc42.** *A*, initial velocity measurements for ATP were obtained using a constant concentration of $Cdc42_{1-179}$Q61L of 500 μM while varying the ATP concentrations from 100 to 10,000 μM. *B*, initial velocity measurements for Cdc42 were obtained at 5 mM ATP while varying the concentration of $Cdc42_{1-179}$Q61L between 100 and 2800 μM. Assays were performed in triplicate with IbpA-Fic2 at 0.56 nM. The *line* represents the fit of this data using the Michaelis-Menten equation ("Experimental Procedures"). *Error bars* indicate S.E.

GDP dissociation stimulators catalyzing the exchange of GDP for GTP, thus activating Rho GTPases. The GTPase-activating proteins enhance the intrinsic ability of the GTP-binding proteins to hydrolyze GTP to GDP, thus inactivating Rho GTPases. Finally, GDIs extract Rho family GTPases from the membrane and inhibit the exchange of GDP for GTP as well as the hydrolysis of GTP. Because crystallographic data indicate that IbpA-Fic2 locks Cdc42 in a conformation that resembles its RhoGDI-bound state (9), we sought to determine whether Rho GTPase-RhoGDI complexes could be adenylylated by IbpA-Fic2. Specifically, HA-tagged RhoA, Rac1, or Cdc42 exchanged with either GDP or GMP-PNP was bound to an Ni^{2+}-NTA-agarose column containing bacterially purified His_6-SUMO-tagged RhoGDI. This column with the Rho GTPase-RhoGDI complex was then subjected to Fic-mediated adenylylation. Following the adenylylation reaction, the supernatant and eluate of the bead (agarose) fractions were separated by SDS-PAGE and analyzed by autoradiography and Ponceau S staining. Fig. 1*C* shows the results with the GDP-loaded Cdc42-RhoGDI complex. The autoradiograph indicates that IbpA-Fic2 is able to adenylylate Cdc42 in a complex with RhoGDI and does not effectively disassociate the complex, as determined by the lack of ^{32}P signal in the supernatant lane. Similar results were obtained for GDP-loaded RhoA and Rac1, as well as with GMP-PNP loaded RhoA, Rac1, and Cdc42 bound to RhoGDI (supplemental Fig. 2*C* and data not shown).

Kinetics of IbpA-Fic2 Activity on Cdc42—Because IbpA-Fic2 efficiently targets activated Cdc42, we performed kinetic analyses on the IbpA-Fic2 ATase activity using a Cdc42-Q61L point mutant that mimics Cdc42 in its active/GTP-bound form (19). This mutant displays greater stability than Cdc42-G12V at the high protein concentrations required for the kinetic analyses (8).

IbpA-Fic2 hydrolyzes ATP to AMP and PP_i, whereas it catalyzes the addition of AMP to the invariant Tyr in the switch 1 region of the Rho GTPases. We used an untagged IbpA-Fic2 construct (composed of amino acids 3482–3797 of IbpA) because tagged versions of Fic2 displayed slightly reduced catalytic efficiency (data not shown). This protein was also used in our previous crystallization studies and is highly active and stable (9). We used untagged $Cdc42_{1-179}$Q61L as a substrate. The last 12 amino acids where removed from the C terminus to aid in solubility. The concentrations of IbpA-Fic2 (0.56 nM) and Cdc42 (500 μM) were constant, whereas the ATP concentration was varied from 0.1 to 10 mM. The apparent K_m for ATP was 0.73 mM ± 0.04 with a K_{cat} of 111 s^{-1} ± 2. The catalytic efficiency (K_{cat}/K_m) for ATP was 1.53×10^5 $M^{-1}s^{-1}$ (Fig. 2). The kinetic constants for Cdc42-Q61L were determined using 0.56 nM IbpA-Fic2 and 5 mM ATP while varying the Cdc42-Q61L from 0.1 to 2.8 mM. The apparent K_m was 1.57 mM ± 0.15, the K_{cat} was 255 s^{-1} ± 15, and the K_{cat}/K_m was 1.72×10^5 $M^{-1}s^{-1}$ (Fig. 2). Although somewhat high, these values are in good agreement with those reported for VopS using His_6-tagged Cdc42-Q61L as a substrate (8).

Survey of Ras Family Rho GTPases as Substrates for IbpA, PfhB2, HYPE, and VopS—RhoA, Rac1, and Cdc42 are members of the Rho family of GTPases, which is a subset of the Ras superfamily (20). Based on protein structure and function, the Ras superfamily of GTPases is traditionally classified into five subfamilies: Ras, Rho, Rab, Arf1, and Ran (20). We, therefore, surveyed several representatives from each subfamily to determine the variety of GTPases that can be targets of Fic-mediated

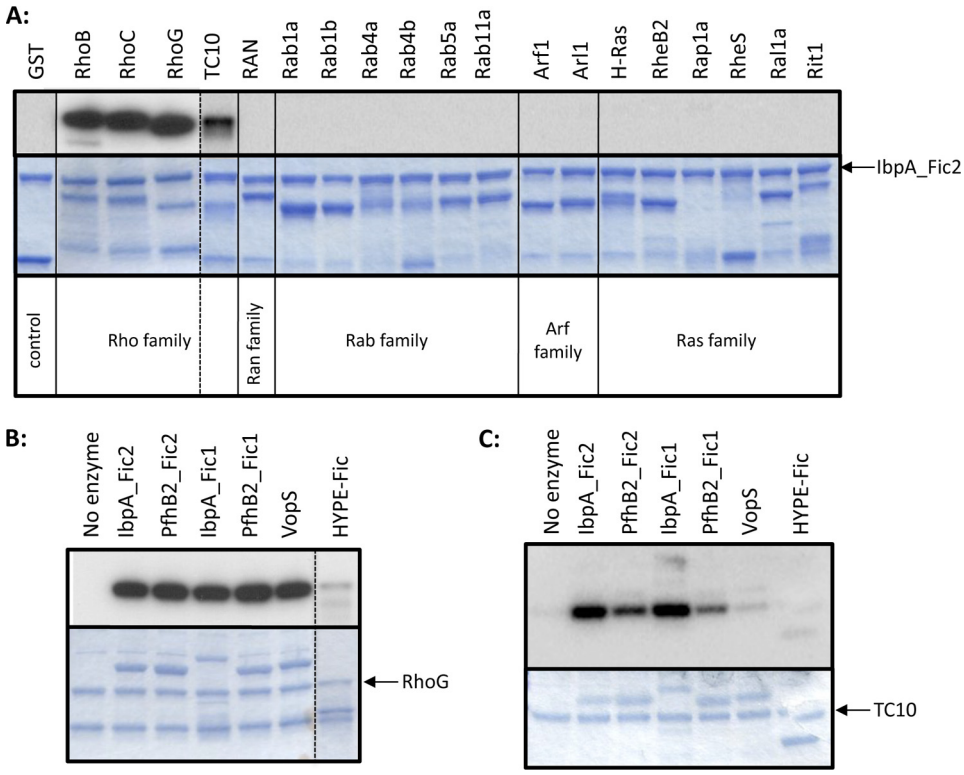

FIGURE 3. **Fic domains of IbpA, PfhB2, and VopS preferentially target the Rho subfamily of GTPases for adenylylation.** *A*, survey of Ras family Rho GTPases as substrates for Fic-mediated adenylylation. The indicated GST-tagged Rho GTPases were bacterially expressed and purified and incubated with purified IbpA-Fic2 in an *in vitro* adenylylation reaction. Samples were separated on SDS-PAGE and visualized by autoradiography (*top panel*) and Coomassie Blue staining (*bottom panel*). The position of IbpA-Fic2 on the gel is indicated by an *arrow*. IbpA-Fic2 adenylylated only the Rho family members, RhoB, RhoC, RhoG, and TC10. *B*, the ability of Fic enzymes to adenylylate RhoG. GST-tagged and purified IbpA-Fic1, IbpA-Fic2, PfhB2-Fic1, PfhB2-Fic2, VopS, and HYPE-Fic were incubated with bacterially expressed and purified GST-RhoG in an *in vitro* adenylylation reaction. Samples separated by SDS-PAGE were visualized by autoradiography (*top panel*) and Coomassie Blue staining (*bottom panel*). The position of RhoG on the gel is indicated by an *arrow*. The Fic domains of IbpA, PfhB2, and VopS efficiently adenylylate RhoG, whereas the Fic domain of HYPE displays a weaker adenylylation activity. *C*, the ability of Fic enzymes to adenylylate TC10. GST-tagged and purified IbpA-Fic1, IbpA-Fic2, PfhB2-Fic1, PfhB2-Fic2, VopS, and HYPE-Fic were incubated with bacterially expressed and purified GST-TC10 in an *in vitro* adenylylation reaction. Samples separated by SDS-PAGE were visualized by autoradiography (*top panel*) and Coomassie Blue staining (*bottom panel*). The position of TC10 on the gel is indicated by an *arrow*. The Fic domains of IbpA and PfhB2 can efficiently adenylylate TC10, whereas VopS shows minimal activity toward it. HYPE did not adenylylate TC10 *in vitro*.

adenylylation. An alignment of the switch 1 region of these GTPases indicates several highly conserved amino acid residues, including an invariant threonine corresponding to Thr-35 of Cdc42 that is adenylylated by VopS (supplemental Fig. 3). Additionally, the Tyr-32 of Cdc42 that is adenylylated by IbpA, PfhB2, and HYPE is conserved in several Rho and Ras proteins (supplemental Fig. 3). We cloned and purified GST-tagged versions of additional Rho (RhoB, RhoC, RhoG, and TC10), Ras (H-Ras, RheB, RheS, Rap1a, Ral1A, and Rit1), Rab (Rab1a, Rab1b, Rab4a, Rab4b, Rab5a, and Rab11a), Arf (Arf1 and Arl1), and Ran (Ran) subfamily members and tested them *in vitro* as substrates for adenylylation by IbpA-Fic1, IbpA-Fic2, PfhB-Fic1, PfhB-Fic2, VopS, or HYPE-Fic (Fig. 3). Surprisingly, only Rho family members RhoB, RhoC, RhoG, and TC10 were adenylylated by any of the Fic enzymes despite high switch 1 sequence conservation and the presence of the invariant Thr-35/37 (Fig. 3*A* and supplemental Fig. 3). Interestingly, although most Rho family members, including RhoG (Fig. 3*B*), were efficiently adenylylated by the various enzymes except HYPE-Fic, TC10 was efficiently adenylylated only by the Fic domains of IbpA and PfhB2 and was only weakly modified by VopS (Fig. 3*C*). Further, HYPE-Fic did not modify TC10, supporting our hypothesis and previous observations that Rho GTPases are not the physiological target(s) of HYPE (Fig. 3*C*) (2). RhoB, RhoC, RhoG, and TC10 belong to the Rho subfamily, which includes RhoA, Rac1, and Cdc42, and display a structural similarity to these GTPases. We, therefore, infer that the Fic domains of IbpA, PfhB2, and VopS preferentially target only the Rho subfamily of GTPases for adenylylation.

Nucleotide Specificity of Fic ATases—We next surveyed the ability of the Fic domains of IbpA, PfhB2, VopS, and HYPE to utilize nucleotides other than ATP while modifying Rho GTPases. Results using the active form of Cdc42 (Cdc42-Q61L) are shown (Fig. 4). Cdc42-Q61L was incubated with Fic enzymes in identical *in vitro* reactions using equal amounts of α-^{32}P-labeled ATP, GTP, CTP, UTP, or dTTP. ATP was the preferred nucleotide source for all the Fic domains tested (Fig. 4*A*). As expected, HYPE-Fic displayed the weakest activity and required longer exposure for detection by autoradiography (Fig. 4*B*). Surprisingly, VopS displayed an equal preference for utilizing ATP or GTP, indicating that VopS may also function as a guanylyltransferase. Additionally, the Fic domains of IbpA, PfhB2, and HYPE displayed a moderate level of activity with CTP, whereas VopS preferred UTP over CTP. Longer exposures indicated that all the Fic enzymes tested could utilize any of the nucleotides to some extent (data not shown).

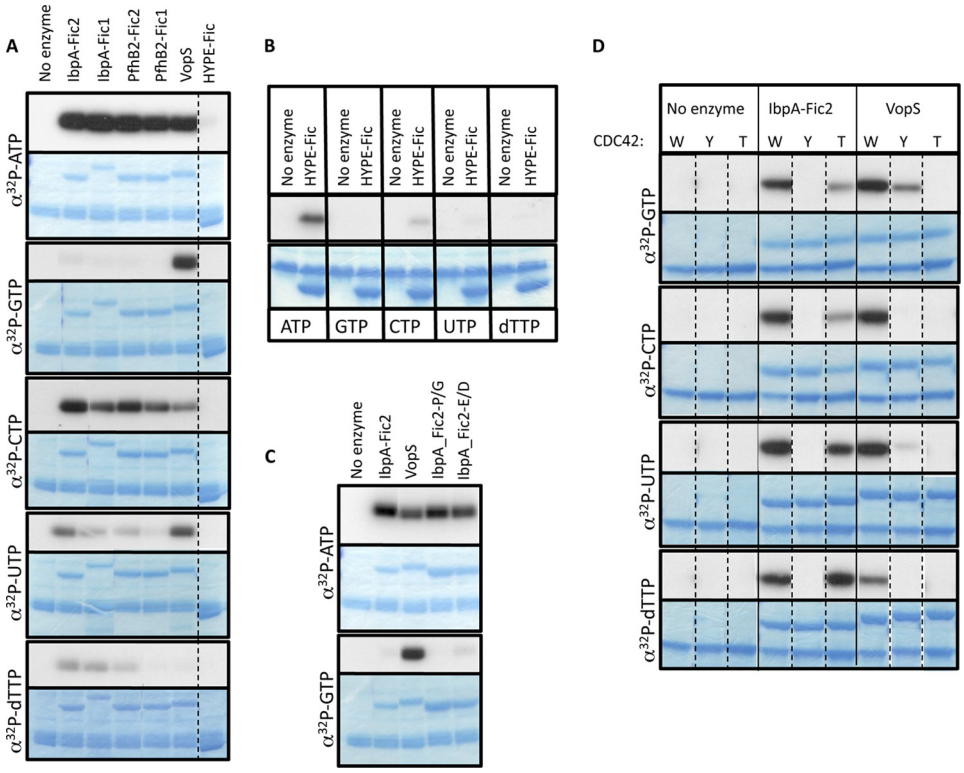

FIGURE 4. **Nucleotide specificity of IbpA-Fic2.** *A*, GST-tagged and purified IbpA-Fic1, IbpA-Fic2, PfhB2-Fic1, PfhB2-Fic2, and VopS and His_6-SUMO-tagged HYPE-Fic were incubated with $Cdc42_{1-179}$Q61L in an *in vitro* reaction using [α-^{32}P]ATP, -GTP, -CTP, -UTP, or -dTTP. Samples separated by SDS-PAGE were visualized by autoradiography (*top panel*) and Coomassie Blue staining (*bottom panel*). The ability of the indicated Fic enzymes to utilize different nucleotides for post-translationally modifying Cdc42 is shown. All the panels were given equal exposure times for autoradiography. The *dotted line* represents a break in the gels. *B*, reactions with His_6-SUMO-tagged HYPE-Fic displayed in *panel A* were rerun on SDS-PAGE and visualized by longer exposures for autoradiography (*upper panel*) and Coomassie Blue staining (*bottom panel*). HYPE-Fic efficiently uses ATP, and CTP to a lesser degree, to modify Cdc42. *C*, point mutations in the IbpA-Fic2 Fic motif did not alter its affinity for nucleotides. GST-tagged and purified Pro-3718 to Gly (IbpA_Fic2-P/G) and Glu-3271 to Asp (IbpA_Fic2-E/D) mutants of IbpA-Fic2, as well as wild type IbpA-Fic2 and VopS, were incubated with Cdc42-Q61L using [α-^{32}P]ATP and -GTP in an *in vitro* reaction. Samples were separated on SDS-PAGE and visualized by autoradiography (*top panel*) and Coomassie Blue staining (*bottom panel*). Conversion of the IbpA-Fic2 Fic motif sequence to match the corresponding residues in the Fic motif of VopS did not confer specificity for nucleotides. *D*, comparison of IbpA-Fic2 and VopS to target switch 1 Tyr-32 and Thr-35 mutants of Cdc42 using different nucleotides. GST-tagged IbpA-Fic2 and VopS were incubated with wild type (*W*), Y32F (*Y*), or T35A (*T*) versions of Cdc42 expressed as GST fusion proteins in bacteria in an *in vitro* assay using [α-^{32}P]ATP, -GTP, -CTP, -UTP, or -dTTP. Samples were assessed by autoradiography (*top panel*) with exposure times adjusted for optimal visualization and by Coomassie Blue staining (*lower panel*). Mutation of T35A in Cdc42 did not alter the ability of IbpA-Fic2 to target the switch 1 Tyr-32 for modification. In contrast, the Y32F mutation in Cdc42 severely impaired VopS in modifying Thr-35 using the different nucleotide sources.

Point mutations in the IbpA-Fic2 Fic motif did not alter its affinity for nucleotides. IbpA-Fic2-P3718G or IbpA-Fic2-E3721D mutations, which mimic the corresponding residues in the Fic motif of VopS, did not confer specificity for GTP (Fig. 4*C*). Thus, the Fic motif sequence alone does not dictate nucleotide specificity.

Finally, we compared the ability of IbpA-Fic2 and VopS to target switch 1 Tyr-32 and Thr-35 mutants of Cdc42 using different nucleotides (Fig. 4*D*). As seen with ATP, IbpA-Fic2 modified the Cdc42-T35A mutant but not Cdc42-Y32F, irrespective of the nucleotide source. In contrast, VopS was impaired in its ability to add CMP, UMP, and dTMP to both the Cdc42-T35A and the Cdc42-Y32F mutants. These results indicate that coordination of nucleotides within the Fic enzymatic pocket depends not just on the Fic enzyme but also on the substrate. We reason that mutations in the switch 1 Tyr-32 induce minor conformational changes in Cdc42, which affect the ability of VopS to target Thr-35. In contrast, mutations in Thr-35 are tolerated by IbpA-Fic2. This synergistic role of the enzyme-nucleotide-substrate complex may be what allows efficient adenylylation by Fic enzymes despite having high K_m values for ATP and Cdc42.

Phylogenetic Analysis of the IbpA Fic Domains—Of the 4300 known Fic proteins that constitute the FiDo family, only IbpA-Fic2 and VopS have previously been enzymatically characterized (2, 8, 12). In addition, the Enzyme Commission (EC) lists several distinct classes of enzymes as ATP-dependent ATases. These include glutamine-synthetase ATases (EC 2.7.7.42), UBA4 E1-ligase activating ATases (EC 2.7.7.53), phenylalanine ATases (EC 2.7.7.54) that target amino acids, polynucleotide ATases (EC 2.7.7.19 and 2.7.7.72), DNA- and RNA-specific ligases (EC 6.5.1), aminoglycoside ATases (EC 2.7.7.46), and sugar-specific ATases (EC 2.7.7.27, 2.7.7.35, and 2.7.7.36) (Fig. 5). All these ATases have evolved to target proteins, nucleotides, and sugars and are involved in diverse biological processes, illustrating the importance of adenylylation in cellular signaling. We reasoned that a phylogenetic analysis of the IbpA Fic domains with these other classes of ATP-dependent ATases might help understand the nature of the FiDo family. We generated a phylogenetic tree for each of the

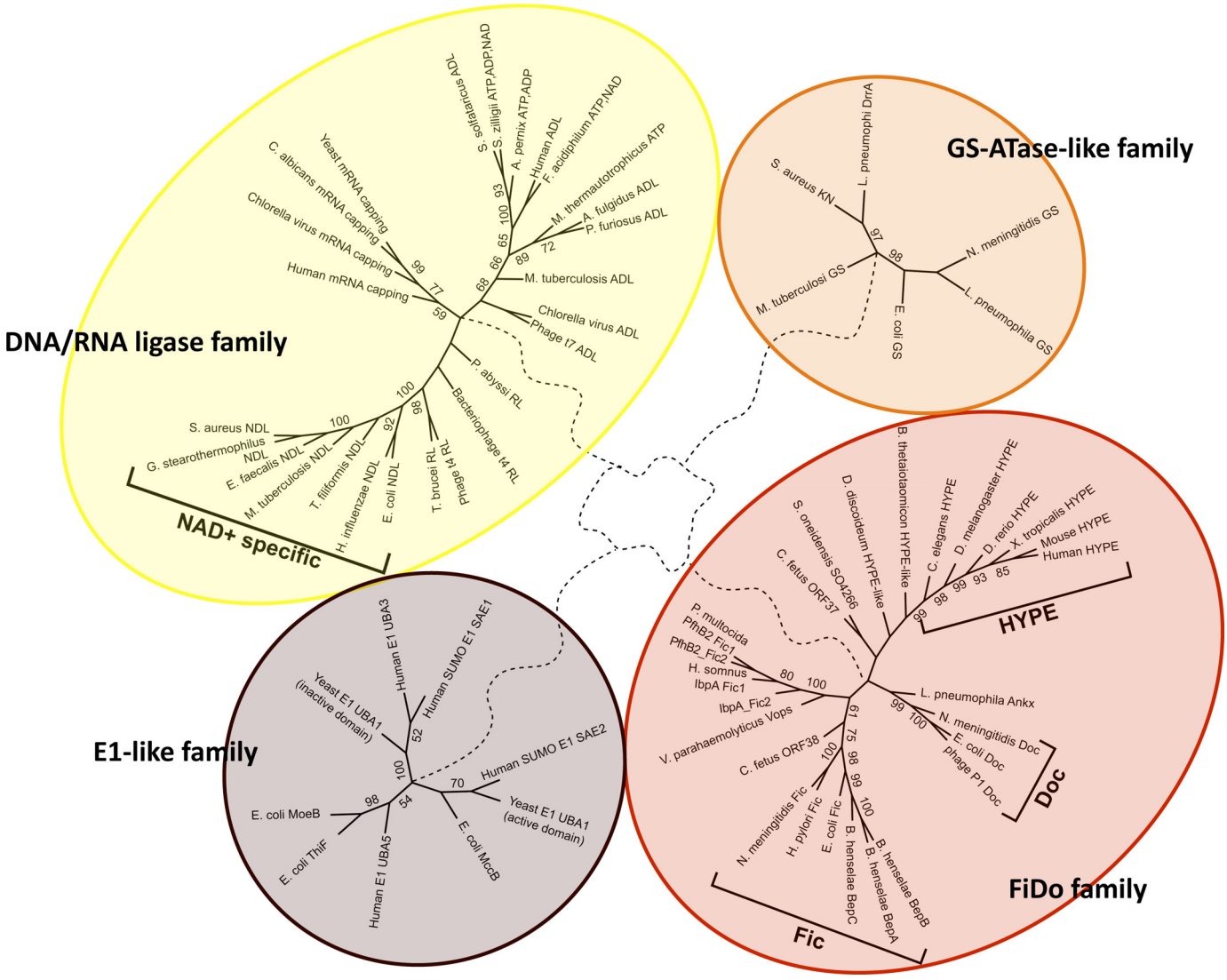

FIGURE 5. **Phylogenetic comparison of Fic enzymes with other classes of adenylyltransferases.** A phylogenetic tree was generated using the neighbor joining method for each of the ATase families using the adenylyltransferase domain of index proteins shown in supplemental Table 1. The four families of ATases are shown: DNA/RNA ligases (in *yellow*) with a *bracket* indicating NAD^+-specific enzymes; the GS-ATase family (in *orange*); the E1 ubiquitin ligase family (in *chocolate brown*); and the FiDo family (in *red*) with *brackets* indicating the HYPE, Doc, and Fic subgroups. *NDL*, NAD^+ dependent ligase; *ADL*, ATP dependent ligase; *RL*, RNA ligase; *KN*, kanamycin nucleotidyltransferase.

ATase families using the adenylyltransferase domain of index proteins shown in supplemental Table 1. ATases appear to have evolved early in life and have been reinvented several times to generate four dominant clades (Fig. 5, *yellow*, *orange*, *red*, and *chocolate ellipses*).

Like each of the ATase families analyzed, the FiDo family appears to have evolved independently from other clades of ATases (Fig. 5). It can be further classified into three main groups: (*a*) Doc, (*b*) HYPE, and (*c*) Fic (Fig. 5, *red ellipse*). The Doc group contains proteins with a Fic motif resembling the bacteriophage P1 Doc HIFNDANKR sequence. These are typically small proteins (125–150 amino acids), lacking any other protein domain, and are often part of a toxin-antitoxin complex (21). The Doc proteins are members of a larger group of proteins classified as the post-segregational cell killing system, which allows plasmids to maintain themselves within their bacterial host (21). The HYPE group consists of a single Fic locus found in each animal genome and has potential orthologs in other eukaryotic lineages as well as in bacteria and archaea. These have a core motif of HPF*XX*GNGR, and all animal members contain a signal peptide and a tetratricopeptide repeat domain. We speculate that the HYPE tetratricopeptide repeat domain is involved in substrate recognition. Many prokaryotic HYPE proteins are associated with helix-turn-helix domains, which may be involved in transcriptional activation. Finally, the Fic group includes *E. coli* Fic and its bacterial homologs. These proteins are generally longer than Doc proteins but are not associated with a post-segregational cell killing system (21). They also do not display a conserved operon architecture, suggesting that they may have evolved to carry out different functions.

Within the Fic family, the IbpA Fic domains branch closely with those of PfhB2, as expected from their nearly 64% amino acid sequence identity (Fig. 5, *red ellipse*). Interestingly, IbpA, PfhB2, and VopS form a distinct clade that branches away from *E. coli* Fic, suggesting that these enzymes may have evolved to

target proteins from their mammalian hosts. A similar divergence is observed for the *L. pneumophila* virulence factor AnkX, which has a non-canonical Fic motif resembling that of P1 bacteriophage Doc (Fig. 5, *red ellipse*). Recently, *L. pneumophila* DrrA was shown to adenylylate a tyrosine residue in the switch 2 region of Rab1b, by an enzymatic mechanism similar to *E. coli* GS-ATase (6). The GS-ATase phylogeny indicates that DrrA diverged away from *E. coli* GS-ATase but retained the ability to utilize ATP to adenylylate a mammalian substrate, possibly due to its intimate association with the human host (Fig. 5, *orange ellipse*). Further, DrrA also guanylylates Rab1b (6). Unlike Fic proteins, adenylylation of Rab1b by DrrA constitutively activates the GTPase (6). It would be interesting to determine whether DrrA and AnkX use adenylylation as a mechanism to counter each other and finely tune the ability of *Legionella* to modulate vesicular trafficking.

Finally, a comparison of the Fic phylogeny with DNA/RNA ligases reveals that although many ATP/ADP/NAD^+-specific ligases cluster together, those that are exclusively NAD^+-specific branch separately from the rest of the family members (Fig. 5, *yellow ellipse*). It remains to be determined whether a nucleotide or NAD^+-specific branch exists within the FiDo family.

Conclusion—By conducting a detailed analysis of the enzymatic, kinetic, and phylogenetic properties of IbpA-Fic2, we have gained important insights into factors that determine substrate specificity for Fic adenylyltransferases. We show that although most of the Fic enzymes tested displayed higher specificity for ATP as a nucleotide source, VopS displayed an equal affinity for GTP. Thus, Fic proteins have the potential to carry out post-translational modifications beyond adenylylation alone. We further demonstrate that nucleotide specificity can be dictated by the enzyme-nucleotide-substrate complex formed during the chemical reaction. Additionally, the IbpA Fic domains can target Rho GTPases both in their active (GTP-bound) as well as in their inactive (GDP-bound and RhoGDI-bound) states, thus preventing their downstream signaling function. It must be noted that unlike the IbpA Fic domains, which target Tyr-32/Tyr-34 of Rac1/Cdc42/RhoA, VopS adenylylates Thr-35/Thr-37 of Rac1/Cdc42/RhoA. Thr-35 of Rac1 has been shown to play a critical role in binding to the regulatory arm of RhoGDI (22). It, thus, remains to be determined whether VopS functions differently than IbpA in its ability to adenylylate Rho GTPases in complex with RhoGDI. We also determined that *Pasteurella* PfhB2 displayed ATase activity similar to the Fic domains of IbpA. Finally, we compared the IbpA-Fic2 kinetic properties with those of VopS and found that the two enzymes display similar affinities for ATP and Cdc42 despite targeting different residues on the Cdc42 substrate. The comparative phylogenetic analysis of Fic proteins with other known nucleotidyltransferases provides a perspective for the chemical diversity observed within the Fic family.

Fic proteins have been implicated in processes as diverse as bacterial pathogenesis, cell division, protein translation, eukaryotic cell signaling, and cellular trafficking. Chemical characterization of these enzymes is essential for providing a unifying, conserved catalytic mechanism to explain these otherwise disparate biological processes.

Acknowledgments—We thank members of the Dixon laboratory for helpful discussions. Special thanks go to Dr. Joseph Adams (University of California, San Diego) for help with analysis of kinetic data and to Dr. Lynette Corbeil (University of California, San Diego) for providing P. multocida genomic DNA.

REFERENCES

1. Tagawa, Y., Sanders, J. D., Uchida, I., Bastida-Corcuera, F. D., Kawashima, K., and Corbeil, L. B. (2005) *Microb. Pathog.* **39,** 159–170
2. Worby, C. A., Mattoo, S., Kruger, R. P., Corbeil, L. B., Koller, A., Mendez, J. C., Zekarias, B., Lazar, C., and Dixon, J. E. (2009) *Mol. Cell* **34,** 93–103
3. Brown, M. S., Segal, A., and Stadtman, E. R. (1971) *Proc. Natl. Acad. Sci. U.S.A.* **68,** 2949–2953
4. Hochstrasser, M. (2009) *Nature* **458,** 422–429
5. Kerscher, O., Felberbaum, R., and Hochstrasser, M. (2006) *Annu. Rev. Cell Dev. Biol.* **22,** 159–180
6. Müller, M. P., Peters, H., Blümer, J., Blankenfeldt, W., Goody, R. S., and Itzen, A. (2010) *Science* **329,** 946–949
7. Zekarias, B., Mattoo, S., Worby, C., Lehmann, J., Rosenbusch, R. F., and Corbeil, L. B. (2010) *Infect. Immun.* **78,** 1850–1858
8. Luong, P., Kinch, L. N., Brautigam, C. A., Grishin, N. V., Tomchick, D. R., and Orth, K. (2010) *J. Biol. Chem.* **285,** 20155–20163
9. Xiao, J., Worby, C. A., Mattoo, S., Sankaran, B., and Dixon, J. E. (2010) *Nat. Struct. Mol. Biol.* **17,** 1004–1010
10. Yarbrough, M. L., Li, Y., Kinch, L. N., Grishin, N. V., Ball, H. L., and Orth, K. (2009) *Science* **323,** 269–272
11. Roy, C. R., and Mukherjee, S. (2009) *Sci. Signal.* **2,** pe14
12. Kinch, L. N., Yarbrough, M. L., Orth, K., and Grishin, N. V. (2009) *PLoS One* **4,** e5818
13. Das, D., Krishna, S. S., McMullan, D., Miller, M. D., Xu, Q., Abdubek, P., Acosta, C., Astakhova, T., Axelrod, H. L., Burra, P., Carlton, D., Chiu, H. J., Clayton, T., Deller, M. C., Duan, L., Elias, Y., Elsliger, M. A., Ernst, D., Feuerhelm, J., Grzechnik, A., Grzechnik, S. K., Hale, J., Han, G. W., Jaroszewski, L., Jin, K. K., Klock, H. E., Knuth, M. W., Kozbial, P., Kumar, A., Marciano, D., Morse, A. T., Murphy, K. D., Nigoghossian, E., Okach, L., Oommachen, S., Paulsen, J., Reyes, R., Rife, C. L., Sefcovic, N., Tien, H., Trame, C. B., Trout, C. V., van den Bedem, H., Weekes, D., White, A., Hodgson, K. O., Wooley, J., Deacon, A. M., Godzik, A., Lesley, S. A., and Wilson, I. A. (2009) *Proteins* **75,** 264–271
14. Palanivelu, D. V., Goepfert, A., Meury, M., Guye, P., Dehio, C., and Schirmer, T. (2011) *Protein Sci.* **20,** 492–499
15. Garcia-Pino, A., Christensen-Dalsgaard, M., Wyns, L., Yarmolinsky, M., Magnuson, R. D., Gerdes, K., and Loris, R. (2008) *J. Biol. Chem.* **283,** 30821–30827
16. Liu, M., Zhang, Y., Inouye, M., and Woychik, N. A. (2008) *Proc. Natl. Acad. Sci. U.S.A.* **105,** 5885–5890
17. Pellegrin, S., and Mellor, H. (2008) in *Current Protocols in Cell Biology*, Vol. 38, pp. 14.8.1–14.8.19, John Wiley & Sons, Inc., New York
18. Jaffe, A. B., and Hall, A. (2005) *Annu. Rev. Cell Dev. Biol.* **21,** 247–269
19. Zhang, X. F., Schaefer, A. W., Burnette, D. T., Schoonderwoert, V. T., and Forscher, P. (2003) *Neuron* **40,** 931–944
20. Wennerberg, K., Rossman, K. L., and Der, C. J. (2005) *J. Cell Sci.* **118,** 843–846
21. Anantharaman, V., and Aravind, L. (2003) *Genome Biol.* **4,** R81
22. Hoffman, G. R., Nassar, N., and Cerione, R. A. (2000) *Cell* **100,** 345–356